Supplementary Material:
End-to-End Conformal Prediction for Trajectory Optimization

Response to Reviewers

Response to Reviewer jfjR Thank you very much for your valuable comments, which have helped us to improve the quality of this manuscript.

> **Question (1):** The paper of Stamouli et al that is cited, which develops a normalized nonconformity score for the TO setting, claims to improve upon the performance of Lindemann et al strategy.

> **Question (1a):** Can it be included in the baselines?

Thank you very much for your valuable comment and suggestion. Following the reviewer's suggestion, we have included the Recursively Feasible MPC using CP (RF-CP) method proposed in [1] as a baseline and conducted comparison with our method on the quadrotor model. We summarize the experiment results as follows. The results demonstrate that our method is superior to RF-CP in terms of average cost and computation time. Specifically, thanks to its proposed normalized nonconformity score, its average cost is comparable to that of E2E-CP-ARA, but it remains 85.8% higher than E2E-CP-IRA. However, the normalized nonconformity score introduces mixed-integer variables into the Trajectory Optimization (TO) problem, significantly increasing the computation time. Specifically, the average computation time of RF-CP is more than an order of magnitude higher than that of E2E-CP-IRA, and significantly exceeds the sampling time (0.125s), making it infeasible for real-time control. For detailed data and analysis of this experiment, we kindly refer the reviewer to Section B of this Supplementary Material.

> **Question (1b):** Can you replace your regression scores in the proposed methods with the normalized regression scores from Stamouli et al and further enhance performance?

Thank you very much for your valuable comment. In fact, one significant advantage of the proposed E2E-CP framework is its flexibility in incorporating other nonconformity scores. Following the reviewer's suggestion, we have incorporated the normalized nonconformity score in [1] into our framework with some modifications and derived the corresponding theoretical results. The specific incorporating method and theoretical results have been added to the appendix of the revised manuscript and Section E of the this Supplementary Material , where the reviewer can refer to for further details. It is important to note that, as described in response to **(1a)**, the normalized nonconformity score introduces mixed-integer variables into the TO problem, which significantly increases the solution time, especially when using the IRA method and dealing with nonlinear systems.

We would like to thank the reviewer for helping us further enrich our paper. We have added an acknowledgment in the revised manuscript to express our gratitude to an anonymous reviewer who proposed this novel idea.

[1] *Stamouli, C., Lindemann, L., and Pappas, G. Recursively feasible shrinking-horizon mpc in dynamic environments with conformal prediction guarantees. In Learning for Dynamics and Control Conference, 2024.*

Question (2): Given the computational tradeoff induced by IRA, which is much more efficient but requires solving a bulky problem each time in contrast to the average allocation, is it possible to adapt the methods into a hybrid method, which runs IRA only on select rounds and the average allocation on the rest? Would such a hybrid method smoothly interpolate the efficiency gain between those two percentages you reported, or would just a few IRA redistributions already lead to a massive efficiency improvement?

Thank you very much for your valuable comment and suggestion. Following the reviewer's suggestion, we have explored this hybrid method. Specifically, we define a switching time ts, such that when $t < t_s$, the IRA method is used, and when $t \geq t_s$, the ARA method is applied. Clearly, when $t_s = 0$ and 20, the hybrid method degenerates to the ARA and IRA method, respectively. We conducted experiments with different switching times ($t_s = 0, 1, 6, 11, 16, 20$) using the kinematic vehicle model. The experiment result shows that using IRA only at the initial time step results in a 66.56% reduction in average cost. This is because the trajectory obtained at the initial time step determines the overall path of the entire trajectory. As ts increases, the average cost naturally decreases. When t_s reaches 11, further increases in ts no longer lead to significant reduction in the average cost. This is because, in our scenario, the interaction between obstacles and the vehicle is most intensive at the middle of the mission time. After $t > 11$, the obstacles and the vehicle have moved apart, significantly reducing the collision risk, which results in ARA and IRA optimizing nearly identical trajectory. In summary, applying IRA only at the initial time step already leads to a significant performance improvement.

Additionally, we investigated the average computation time of IRA at each time step. Specifically, compared with ARA, the majority of the additional computational burden introduced by IRA also arises at the initial time $t = 0$, where it is used to obtain the initial risk allocation and initial trajectory. As a result, although the application of IRA only at the initial time step results in a significant performance improvement, it is also the primary source of increased computation time.

The specific details and thorough discussions of all the experiments mentioned above have been added to Appendix of the revised manuscript and Section C of this Supplementary Material, where the reviewer can refer to for further details.

We have added an acknowledgment in the revised manuscript to express our sincere gratitude to an anonymous reviewer who proposed the novel idea of this hybrid method.

Response to Reviewer FimN Thank you very much for your valuable comments, which have helped us to improve the quality of this manuscript.

Weaknesses: The framework relies on strong assumptions (e.g., data exchangeability) that could limit its practical applicability.

Other Comments Or Suggestions (3): Clarify assumptions regarding data exchangeability and independence, possibly discussing how violations might affect results.

Questions (2): How does the iterative risk allocation perform when the data deviates from the i.i.d. assumption or experiences distribution shifts?

Thank you very much for your valuable comment. We will first demonstrate that the assumption of data exchangeability and independence is not restrictive and holds in many cases. Furthermore, we experimentally demonstrate that the proposed method exhibits a certain degree of robustness to moderate distribution shifts (beyond exchangeability) and can maintain safety and high performance in realistic scenarios (beyond independence).

In Section 3.1, the assumption of data exchangeability and independence between calibration trajectories and test trajectories is derived from Assumption 3.1 (lines 135-136) and Assumption 3.2 (lines 137-140). We will demonstrate that these two assumptions are not restrictive in practice as follows:

1. Assumption 3.1 posits that the system does not influence the real joint obstacle trajectory, which holds approximately in many robotic applications, e.g., autonomous vehicles behave in ways that result in socially acceptable trajectories without changing the behavior of pedestrians [1].

2. Assumption 3.2 assumes the availability of the training and calibration datasets, which is also not restrictive in practice, as extensive data can be sourced from advanced high-fidelity simulators or robotic applications like autonomous vehicles, where datasets are increasingly accessible.

Although many scenarios approximately satisfy our assumptions, we acknowledge that the system state x may change D during test time, e.g., when a robot is too close to a pedestrian. However, in Appendices D and E of the original manuscript, we have demonstrated through analysis and experiments that the proposed method exhibits a certain degree of robustness to moderate distribution shifts and can maintain safety and high performance in realistic scenarios (beyond independence).

Performance on distribution shift (beyond exchangeability)

Specifically, in Appendix D of the original manuscript, we conducted experiments to evaluate the performance of our method under different levels of distribution shift (beyond exchangeability). The experimental results indicate that under moderate distribution shifts, the proposed method can still satisfy the total risk tolerance constraint while maintaining an average cost reduction of at least 57.1%. We would like to further clarify that when the distribution shifts become excessively large, the proposed method inevitably exceeds the total risk tolerance. However, reference [2] explicitly checked through experiments that interactions among agents in multi-agent systems do not introduce large distribution shifts. The reviewer can find the detailed experiment setting, results (Table 6), and the analysis in Appendix D of the original manuscript.

Performance on distribution shift (beyond independence)

Furthermore, in Appendix E of the original manuscript, we also present experiments where the system and obstacles are interdependent. Specifically, the obstacles' avoidance behavior for the system (beyond independence) is incorporated to simulate realistic scenarios. The experiment results indicate that the influence of the system on obstacles indeed reduces the overall collision avoidance rate, as it disrupts the exchangeability between the test and calibration trajectories. However, the reduction in the collision avoidance rate is negligible and remains well within the corresponding total risk tolerance. Moreover, the dependence between the system and obstacles has almost no impact on the average cost empirically. In summary, the experiment results show that interactions among agents in multi-agent systems do not introduce large distribution shifts and will not significantly affect our algorithm and its performance. The reviewer can find the detailed results (Table 7) and the analysis of the experiment in Appendix E of the original manuscript.

In summary, the robustness of our proposed method to distribution shifts is sufficient to handle practical scenarios. Under moderate distribution shifts and dependencies, the proposed method can still ensure that the collision probability does not exceed the given threshold while maintaining nearly unchanged performance. Additionally, in Appendix G of the original manuscript, we discuss several potential ways to address the distribution shift in full generality or to provide theoretical guarantees.

[1] *Lars Lindemann, Matthew Cleaveland, Gihyun Shim, and George J Pappas. Safe planning in dynamic environments using conformal prediction. IEEE Robotics and Automation Letters, 2023.*

[2] *Kegan J Strawn, Nora Ayanian, and Lars Lindemann. Conformal predictive safety filter for rl controllers in dynamic environments. IEEE Robotics and Automation Letters, 2023.*

Other Comments Or Suggestions (1): Correct minor typos (e.g., "Intorduction" should be "Introduction").

Thank you very much for pointing out the typos. We have corrected this minor typo in the revised manuscript and carefully double-checked the manuscript throughout and corrected the edit errors we found.

Other Comments Or Suggestions (2): Consider including a summary diagram or flowchart to illustrate the iterative risk allocation process.

Thank you very much for your valuable comment. In fact, due to space limitations, the pseudocode of the Iterative Risk Allocation (IRA) algorithm was added in Appendix B of the original manuscript. Following the reviewer's suggestion, we have additionally included a flowchart of the IRA algorithm in Appendix B of the revised manuscript. The revised Appendix B has been added to the this Supplementary Material as Section A, where we kindly refer the reviewer to for further details.

Other Comments Or Suggestions (4): Some sections could benefit from simplified language or additional explanatory text to help non-specialists follow the methodology more easily.

Thank you very much for your valuable comment. Following the reviewer's suggestion, we have added some explanatory text and informal (simplified) description of the method to improve the readability of the paper. First, we have added the informal meanings in parentheses to each Lemma, Theorem, and Corollary, for example, "Lemma 4.1. (chance constraint)", "Lemma 4.2. (posterior probability calculation)", "Corollary 4.3. (upper bound of β_τ)", "Lemma 5.1. (monotonicity of J^*)", "Lemma 5.2. (constraint tightening)", and "Theorem 5.3. (convergence guarantee)". Additionally, due to the numerous mathematical notations in the IRA algorithm presented in Section 5, we have included a simplified explanation of the IRA algorithm based on its pseudocode (flowchart) in Appendix B of the revised manuscript to enhance its readability. The revised Appendix B has been added to this Supplementary Material as Section A, where we kindly refer the reviewer to for further details.

Questions (1): How sensitive is the posterior probability calculation method to the particular random split between calibration subsets D1 and D2, and could repeated random splits or cross-validation yield more stable or improved performance?

Thank you very much for your valuable comment and suggestion. Following the reviewer's suggestion, we conducted additional experiments to investigate the sensitivity of the proposed E2E-CP framework to the partitioning of the calibration set. Specifically, we conducted 10 experiments with E2E-CP using the kinematic vehicle model, where the subsets D_{cal}^1 and D_{cal}^2 were randomly split anew. For the ten random experiments, the standard deviation of the average cost is 0.643, and the coefficient of variation is 4.2%, indicating relatively low volatility. For the collision avoidance rate, its volatility is only 2.3%, and all values do not exceed the given tolerance. Therefore, the proposed method is insensitive to the calibration set division. The detailed experiment data can be found in Section D of this Supplementary Material, which we kindly refer the reviewer to.

Questions (3): What is the computational trade-off when scaling the iterative risk allocation method to real-time, high-dimensional trajectory optimization?

Thank you very much for your valuable comment. First, we would like to clarify that we have conducted simulation experiments on a 12-dimensional quadrotor model, which can be found in Appendix C.2 of the original manuscript. The experimental results show that the longest average computation time of E2E-CP-IRA is 0.039s, which is significantly smaller than the sampling time (0.125s), making it fully suitable for real-time control.

Additionally, we conducted a separate analysis of the average computation time of the E2E-CP-IRA at each time step. The experiment results show that the majority of the additional computational burden introduced by IRA arises at the initial time $t = 0$, where it is used to obtain the initial risk allocation and initial trajectory. At subsequent time steps, by using the optimal solution from the previous time step (or iteration) as the initial value for the next time step (or iteration), the IRA algorithm can converge quickly. It is important to note that the TO problem at the initial time step can be solved offline, while the average computation time for TO at subsequent time steps is much smaller than the sampling time. Therefore, E2E-CP-IRA is well-suited for real-time TO. The detailed experiment data can be found in Section C of this Supplementary Material, which we kindly refer the reviewer to.

Response to Reviewer e2g4 Thank you very much for your valuable comments, which have helped us to improve the quality of this manuscript.

Experimental Designs Or Analyses (1): Full or partial calibration data for Lindemann et al., 2023 baseline? The evaluation criteria and baselines appear to mostly make sense. However, given that a main limitation of the proposed method is that it requires splitting the available calibration data into D^1_{cal} and D^2_{cal}–whereas the main baseline from Lindemann et al., 2023 would not require an additional data split, because it is not trying to leverage the feedback information–it should be clarified whether, in the experiments, the baseline from Lindemann et al., 2023 is only calibrated onD^1_{cal}, or whether its CP regions are calibrated using both D^1_{cal} and D^2_{cal}. In my view, a more rigorous evaluation would compare to the baseline calibrated on both D^1_{cal} and D^2_{cal}, because that baseline does not require this further data split.

Questions (1): My question "Full or partial calibration data for Lindemann et al., 2023 baseline?" in the "Experimental Designs Or Analyses" section.

Thank you very much for your valuable comment. In fact, the baseline method [1] simultaneously utilizes the data from both sets D^1_{cal} and D^2_{cal} for generating CP regions in the original manuscript. Specifically, the calibration set D contains a total of 10,000 data points. In our method, we divide the calibration set into D^1_{cal}, containing 2,000 data points, and D^2_{cal}, containing 8,000 data points, where D^1_{cal} is used to obtain the CP regions, and D^2_{cal} is used to calculate the posterior probability. In contrast, the baseline method [1] utilizes the entire calibration set D to obtain the CP regions. We fully agree that the wording in the original manuscript was not very clear and could lead to misunderstandings. Therefore, we have revised the description in the experiment section to clearly indicate that the baseline method [1] uses the complete dataset D.

[1] *Lars Lindemann, Matthew Cleaveland, Gihyun Shim, and George J Pappas. Safe planning in dynamic environments using conformal prediction. IEEE Robotics and Automation Letters, 2023.*

Experimental Designs Or Analyses (2): Other baselines? Additionally, it's possible there may be other baselines that should be compared to–for instance, the experimental setting from Lekeufack et al., 2024 is used for evaluation, but the method from that paper is not compared against or discussed in the related work. In my view this should at least be explained and justified in the related work and experiments section, and/or the method from Lekeufack et al., 2024 should be compared to. A setting from Dixit et al., 2023 also appears to be used, though its baseline (that uses ACI CP) does not appear to be included; however, this may be okay because Dixit et al., 2023 is at least mentioned in the related work.

Thank you very much for your valuable comment. Following the reviewer's valuable suggestion, we have added more comparisons with three additional baseline methods in the quadrotor model: Conformal Control (CC) proposed in [1], Adaptive Conformal Inference for Motion Planning (ACI-MP) proposed in [2], and Recursively Feasible MPC using CP (RF-CP) proposed in [3]. These comparative results convincingly demonstrate the advantages of the proposed method. Specifically, the experiment results show that the average costs of CC and ACI-DP are 296% and 184% higher than that of the proposed method (E2E-CP-IRA), respectively. However, it should be noted that, in practice, CC and ACI-MP are better suited for scenarios where the test data exhibit distribution shift, rather than the setup considered in this experiment. Although the average cost of RF-CP is comparable to that of E2E-CP-ARA, it remains 85.8% higher than E2E-CP-IRA. Additionally, the average computation time of RF-CP is more than an order of magnitude higher than that of E2E-CP-IRA and significantly exceeds the sampling time (0.125s), making it infeasible for real-time control. For detailed data and analysis of the additional baseline experiments, we kindly refer the reviewer to Section B of this Supplementary Material.

[1] *Lekeufack, J., Angelopoulos, A. N., Bajcsy, A., Jordan, M. I., and Malik, J. Conformal decision theory: Safe autonomous decisions from imperfect predictions. In 2024 IEEE International Conference on Robotics and Automation (ICRA), 2024.*

[2] *Dixit, A., Lindemann, L., Wei, S. X., Cleaveland, M., Pappas, G. J., and Burdick, J. W. Adaptive conformal prediction for motion planning among dynamic agents. In Learning for Dynamics and Control Conference, 2023.*

[3] *Stamouli, C., Lindemann, L., and Pappas, G. Recursively feasible shrinking-horizon mpc in dynamic environments with conformal prediction guarantees. In Learning for Dynamics and Control Conference, 2024.*

Essential References Not Discussed: The paper is motivated by improving decision-making with CP and addressing feedback-loops that present when allowing decisions to inform CP regions (e.g., in Intro it is stated there is a "pressing research need" to fill this "research gap"; however, there are several key references addressing these challenges that are not cited, and in my view should be at least mentioned in the Related Work; additionally, at the end I've listed a few other references that are less essential, but are relevant and may be of interest to the authors in future work.

Questions (2): In the "Essential References Not Discussed" section, my points about how at least four key references (on CP+decision making or CP+feedback-loop shifts) should at least be mentioned in the related work

We greatly appreciate the reviewer's suggestion to cite the missing references in the Related Work. Following the reviewer's valuable suggestion, we have added a new subsection titled "Decision-making with CP" in the "Related work" section, where we cite and summarize the four essential references mentioned above.

Action:

Action:Decision-making with CP

Owing to its coverage guarantee and low computational complexity, many studies have focused on the integration of CP with decision-making. [1] was the first to apply CP to decision-making. Additionally, [2] proposed a CP with coverage guarantee under one-step Feedback Covariate Shift (FCS), in which the test data depend on the training data. Building upon the aforementioned work,[3] refined its theoretical framework and extended it to multistep FCS. Furthermore, [4] introduced a conformal decision theory, which follows the ACI concept to directly provide provable statistical guarantees of having low risk for decisions made based on uncertainty-aware predictions.

Additionally, we greatly appreciate the reviewer for providing references that may be helpful for our future work. We have cited the relevant references in the Appendix G (Limitation) of the revised manuscript to assist readers who may be interested in our work.

[1] *Vovk, V. and Bendtsen, C. Conformal predictive decision making. In Conformal and Probabilistic Prediction and Applications, 2018.*

[2] *Fannjiang, C., Bates, S., Angelopoulos, A. N., Listgarten, J., and Jordan, M. I. Conformal prediction under feedback covariate shift for biomolecular design. Proceedings of the National Academy of Sciences, 2022*

[3] *Prinster, D., Stanton, S. D., Liu, A., and Saria, S. Conformal validity guarantees exist for any data distribution (and how to find them). In International Conference on Machine Learning, 2024.*

[4] *Lekeufack, J., Angelopoulos, A. N., Bajcsy, A., Jordan, M. I., and Malik, J. Conformal decision theory: Safe autonomous decisions from imperfect predictions. In IEEE International Conference on Robotics and Automation (ICRA), 2024.*

Weaknesses (1): The authors should use citet for references that are referred to explicitly in the text, and citep for those not.

Thank you very much for your valuable suggestion. Following the reviewer's suggestion, we have made the corresponding revisions to the citations throughout the manuscript.

Weaknesses (2): The methods section gets very dense with math, and can be hard to read. For a final version, it would be good for the authors to revise for readability there, eg double-checking that each new term is explained as it is introduced (eg, in Lemma 4.1, I think this is the first time I saw "LC" as a term, though it isn't explained how it differs from "C" until later, I think). Parentheses to explain the informal meaning of the Lemmas and Theorem would be helpful, eg, "Lemma 4.1 (chance constraint)..."

Thank you very much for your valuable comment. First, we would like to clarity that the symbol L is derived from "the constraint function c is L-Lipschitz continuous" in line 111 of the original manuscript. We fully agree that the introduction of the symbol L and its use in Lemma 4.1 are too distant, which makes the reading difficult. Therefore, we have reiterated the source of L in Lemma 4.1. Following the reviewer's suggestion, we have carefully double-checked the manuscript to

address the issues of unexplained symbols and the concerns mentioned above. Additionally, we have added the informal meanings in parentheses to each Lemma, Theorem, and Corollary as follows.

"Lemma 4.1. (chance constraint)", "Lemma 4.2. (posterior probability calculation)", "Corollary 4.3. (upper bound of β_τ)", "Lemma 5.1. (monotonicity of J^*)", "Lemma 5.2. (constraint tightening)", and "Theorem 5.3. (convergence guarantee)".

> **Questions:** Because my question/concern (1) is about whether the main baseline is properly implemented for a fair comparison and (2) is about essential references that are closely related to the framing and core contribution of the paper, and thus should be mentioned in related work to understand what this paper contributes, I do not think I can recommend accepting this paper in the current form. However, I think these questions are addressable, and if they're resolved, I would be very likely to improve my evaluation of the paper, as I think that the paper does make valuable and useful contributions.

Thank you very much for your insightful and valuable comments. (1) The main baseline method utilizes the full calibration dataset (D^1_{cal} and D^2_{cal}) to generate CP regions, making it a fair comparison. (2) We have cited and discussed the four aforementioned essential references closely related to our framework and discussed their core contributions in the Related Work section of the revised manuscript. Additionally, we have also cited the relevant references provided by the reviewer, which may be helpful for our future work, in the Appendix G (Limitation) of the revised manuscript to assist readers who are interested in our work. Finally, we sincerely appreciate the reviewer's recognition of our work and the valuable suggestions, which have helped us further enhance our work.

A. Details of the E2E-CP-IRA algorithm

The algorithm of E2E-CP using IRA at time t is delineated in Algorithm S.1, and its flowchart is shown in Figure S.1. Note that at time $t = 0$, the input parameter $\alpha_{0:T}$ is initialized as $\alpha_0 = 0,\ \alpha_{1:T} = \alpha/T$, $\beta_{0:t-1}$ is omitted, and the posterior probability calculation in Line 4 is replaced by the assignment $\beta_0 = 0$. ϵ is a given small tolerance. At time t, the robot first obtains the current system state x_t and the joint obstacle states Y_t (Line 2). Then, based on the currently observed joint obstacle states $Y_0, ...Y_t$, the future joint obstacle states $\hat{Y}_{t+1|T}, ..., \hat{Y}_{T|t}$ are predicted using LSTMs (Line 3). Additionally, based on x_t and D^2_{cal}, the posterior collision risk can be calculated through (9) (Line 4). After initialization (Line 5), IRA jointly optimizes risk allocation and trajectory through iteration (Line 6-12). Specifically, in each iteration, IRA first computes the optimal control $u^n_{t:T-1}$, state $x^n_{t+1:T}$, and cost $J^*(\alpha^n_{t+1:T})$ for the current iteration based on the risk allocation $\alpha^n_{t+1:T}$ obtained from the previous iteration (Line 7). The active and inactive constraint sets $\mathcal{I}_{act},\ \mathcal{I}_{ina}$ are determined based on the optimal state $x^n_{t+1:T}$ (Line 8). And then, by sequentially applying the inactive constraint tightening (17) (Line 9) and the redundant risk reallocation (19) (Line 10), the updated risk allocation $\alpha^{n+1}_{t+1:T}$ is obtained. Finally, if the convergence condition is satisfied, the optimal control $u^{n-1}_{t:T-1}$ and the risk allocation $u^{n-1}_{t+1:T}$ are output; otherwise, the next iteration begins (Line 12).

Algorithm S.1 E2E-CP using IRA at time t

1: **Input:** α, $\alpha_{t:T}$, $\beta_{0:t-1}$, ϵ, η, D^1_{cal}, D^2_{cal}
2: Observe the system state x_t and joint obstacle states Y_t
3: $\hat{Y}_{t+1|t}, ..., \hat{Y}_{T|t} \leftarrow$ Trajectory prediction using LSTMs based on $Y_0, ..., Y_t$
4: $\beta_t \leftarrow$ Posterior probability calculation (9) ▷ Using x_t and D^2_{cal}
5: $J^*(\alpha^{-1}_{t+1:T}) \leftarrow \infty$, $\alpha^0_{t+1:T} \leftarrow \alpha_{t+1:T}$, $n \leftarrow 0$ ▷ Initialization of IRA
6: **repeat**
7: $\quad J^*(\alpha^n_{t+1:T}),\ x^n_{t+1:T},\ u^n_{t:T-1} \leftarrow$ Solve the lower-stage problem (12) with $\alpha^n_{t+1:T}$
8: $\quad \mathcal{I}_{act},\ \mathcal{I}_{ina},\ N_{act} \leftarrow$ Identification of active and inactive constraints
9: $\quad \widetilde{\alpha}^n_{t+1:T} \leftarrow$ Transitional risk allocation calculation (17)
10: $\quad \alpha^{n+1}_{t+1:T} \leftarrow$ New risk allocation calculation (19)
11: $\quad n \leftarrow n + 1$
12: **until** $|J^*(\alpha^{n-1}_{t+1:T}) - J^*(\alpha^{n-2}_{t+1:T})| < \epsilon$
13: **Output:** $\beta_{0:t}$, $u^{n-1}_{t:T-1}$, $\alpha_{t+1:T} = \alpha^{n-1}_{t+1:T}$

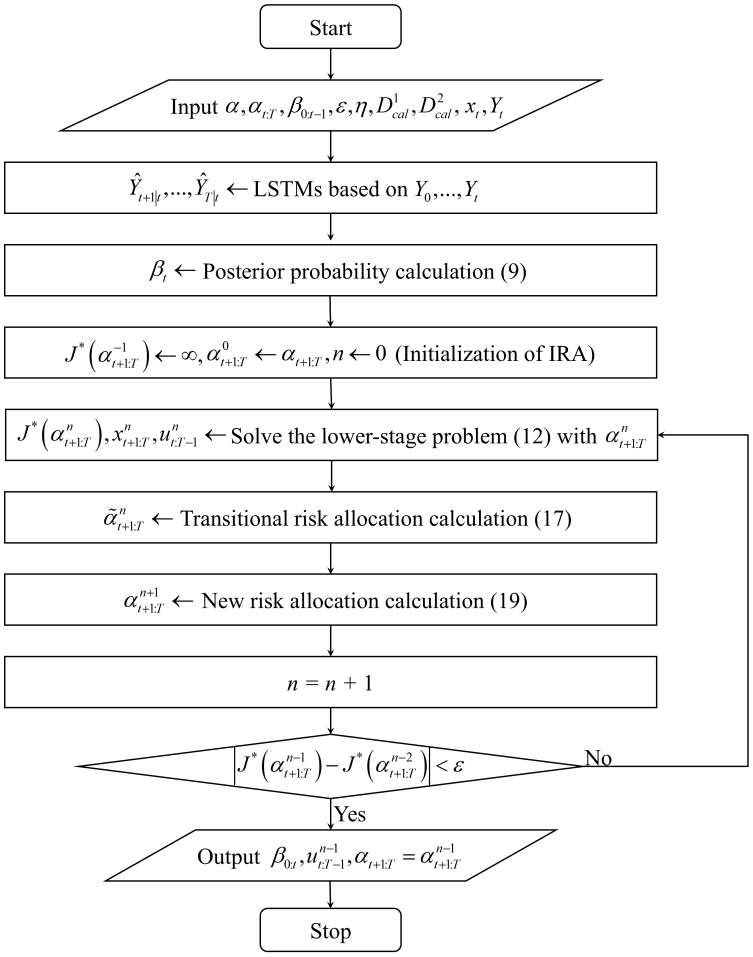

Figure S.1. Flowchart of Algorithm 1.

B. Simulations with additional baselines

We examine the quadrotor model (Dixit et al., 2023) with the following linear dynamics.

$$\begin{aligned} \ddot{x} &= g\theta & \ddot{y} &= -g\phi & \ddot{z} &= \tfrac{1}{m_Q} u_1 \\ \ddot{\phi} &= \tfrac{l_Q}{I_{xx}} u_2 & \ddot{\theta} &= \tfrac{l_Q}{I_{yy}} u_3 & \ddot{\psi} &= \tfrac{l_Q}{I_{zz}} u_4 \end{aligned} \tag{S1}$$

where $g = 9.81$ represents the gravitational acceleration, $m_Q = 0.65$ denotes the mass, and $l_Q = 0.23$ is the distance between the quadrotor and the rotor. $I_{xx} = 0.0075$, $I_{yy} = 0.0075$, and $I_{zz} = 0.013$ correspond to the area moments of inertia about the principle axes in the body frame. The states are the position and orientation with the corresponding velocities and rates — $(x, y, z, \dot{x}, \dot{y}, \dot{z}, \phi, \theta, \psi, \dot{\phi}, \dot{\theta}, \dot{\psi}) \in \mathbb{R}^{12}$. The control inputs u_1, u_2, u_3, u_4 correspond to the thrust force in the body frame and three moments. The system (S1) is discretized using the sampling time $\Delta = 0.125$, and the total time is set to $T = 20$. The objective is to control the quadrotor to reach the target point p_{tar} while navigating around $M = 3$ moving obstacles. We randomly generate 13,000 joint obstacle trajectories and randomly divide them into training D_{train}, calibration D_{cal}, and test D_{test} datasets with the set sizes 2,000, 10,000, and 1,000, respectively. We train an LSTM (Alahi et al., 2016) using D_{train} as the trajectory predictor. For the proposed E2E-CP, D_{cal} is further divided into D^1_{cal} and D^2_{cal} with sizes $|D^1_{cal}| = 2,000$ and $|D^2_{cal}| = 8,000$. We conduct 1,000 Monte Carlo simulations using D_{test}. The following state-of-art methods recently proposed in the literature are analyzed through 1,000 Monte Carlo simulations.

(i) Conformal Control (CC) proposed in Lekeufack et al. (2024).
(ii) ACI for Motion Planning (ACI-MP) proposed in Dixit et al. (2023).
(iii) Recursively Feasible MPC using CP (RF-CP) proposed in Stamouli et al. (2024)

(iv) Sequential CP (S-CP) proposed in Lindemann et al. (2023). Computation of the CP region and TO is performed sequentially.
(v) E2E-CP with ARA (E2E-CP-ARA): The method based on E2E-CP using average risk allocation.
(vi) E2E-CP with IRA (E2E-CP-IRA): The method based on E2E-CP using iterative risk allocation.

Table S.1. Average cost, computation time, and collision avoidance rate using the quadrotor model with different methods (η is the learning rate of CC).

		CC		ACI-MP	RF-CP	S-CP	E2E-CP	
							with ARA	with IRA
Average cost	$\eta = 1000$	59.248	$\alpha = 0.05$	17.970	15.794*	17.321	15.356	7.189
	$\eta = 500$	47.506	$\alpha = 0.10$	17.263	14.378*	16.168	14.228	6.798
	$\eta = 100$	22.459	$\alpha = 0.15$	16.096	11.922*	14.835	12.354	6.191
	$\eta = 50$	21.344	$\alpha = 0.20$	15.310	10.032*	13.217	10.222	5.398
Average computation time	$\eta = 1000$	0.019	$\alpha = 0.05$	0.022	0.487	0.022	0.027	0.038
	$\eta = 500$	0.019	$\alpha = 0.10$	0.026	0.494	0.020	0.021	0.039
	$\eta = 100$	0.021	$\alpha = 0.15$	0.021	0.545	0.021	0.020	0.037
	$\eta = 50$	0.022	$\alpha = 0.20$	0.022	0.500	0.020	0.019	0.036
Collision avoidance rate	$\eta = 1000$	97.0%	$\alpha = 0.05$	98.6%	98.7%	98.8%	98.2%	96.3%
	$\eta = 500$	92.8%	$\alpha = 0.10$	93.3%	96.9%	93.5%	94.6%	94.1%
	$\eta = 100$	82.5%	$\alpha = 0.15$	91.5%	92.4%	92.0%	90.2%	91.9%
	$\eta = 50$	79.1%	$\alpha = 0.20$	87.9%	90.0%	88.2%	86.7%	88.2%

* Until the value obtained after the TO problem converges, with the time far exceeding the sampling time (0.125s).

Table S.1 shows the average cost, average computation time, and collision avoidance rate of 1,000 simulations using the quadrotor model with different methods. Benefiting from the feedback information of posterior probabilities, the average cost of E2E-CP-ARA shows a reduction of at least 11.35% compared to S-CP. Furthermore, by flexibly allocating the allowable risk provided by posterior probabilities, the average cost of E2E-CP-IRA exhibits a significant reduction compared with S-CP. Since the calculation of posterior probabilities does not incur additional computational burden, the average computation time of E2E-CP-ARA is essentially comparable to that of S-CP. Additionally, since CC and ACI-MP fail to fully utilize the information in the calibration dataset, they incur higher costs, which are 296% and 184% higher than that of E2E-CP-IRA, respectively. Particularly for CC, it directly controls the collision avoidance rate by adjusting the weight of the collision penalty term in the objective function, which results in a higher average cost. However, it should be noted that, in practice, CC and ACI-MP are better suited for scenarios where the test data exhibit distribution shift, rather than the setup considered in this section. For RF-CP, thanks to the proposed normalized nonconformity score, its average cost is comparable to that of E2E-CP-ARA, but it remains 85.8% higher than E2E-CP-IRA. However, the normalized nonconformity score introduces mixed-integer variables into the TO problem, significantly increasing the computation time. As shown in Table S.1, the average computation time of RF-CP is more than an order of magnitude higher than that of E2E-CP-IRA and significantly exceeds the sampling time (0.125s), making it infeasible for real-time control. It is worth noting that the proposed framework can also be extended to use this normalized nonconformity score, as detailed in Section E.

C. Computation time of IRA and a hybrid method of ARA and IRA

Table S.2 shows the average computation time at each time t using the kinematic vehicle model with E2E-CP-IRA ($\alpha = 0.2$). It can be observed that, in practice, the majority of the additional computational burden introduced by IRA arises at the initial time $t = 0$, where it is used to obtain the initial risk allocation and initial trajectory. At subsequent time steps, by using the optimal solution from the previous time step (or iteration) as the initial value for the next time step (or iteration), the IRA algorithm can converge quickly. It is important to note that the TO problem at the initial time step can be solved offline, while the average computation time for TO at subsequent time steps is much smaller than the sampling time ($0.125s$). Therefore, E2E-CP-IRA is well-suited for real-time TO.

Furthermore, we explore a hybrid method of ARA and IRA to achieve a trade-off between average cost and average

Table S.2. Average Computation Time (ACT) at each time t using the kinematic vehicle model with E2E-CP-IRA ($\alpha = 0.2$).

t	0 (offline)	1	2	3	4	5	6	7	8	9
ACT	2.3016	0.0348	0.0331	0.0316	0.0277	0.0255	0.0239	0.0220	0.0214	0.0217
t	10	11	12	13	14	15	16	17	18	19
ACT	0.0153	0.0110	0.0093	0.0086	0.0079	0.0070	0.0058	0.0050	0.0049	0.0019

computation time. Specifically, we define a switching time t_s, such that when $t < t_s$, the IRA method is used, and when $t \geq t_s$, the ARA method is applied. Table S.3 shows the average cost and computation time using the kinematic vehicle model with different switching time t_s ($\alpha = 0.2$). It can be observed that using IRA only at the initial time step results in a 66.56% reduction in average cost. This is because the trajectory obtained at the initial time step determines the overall path of the entire trajectory. As t_s increases, the average cost naturally decreases. When t_s reaches 11, further increases in t_s no longer lead to significant reduction in the average cost. This is because, in our scenario, the interaction between obstacles and the vehicle is most intensive at the middle of the mission time. After $t > 11$, the obstacles and the vehicle have moved apart, significantly reducing the collision risk, which results in ARA and IRA optimizing nearly identical trajectory. Although the aforementioned hybrid method balances the trade-off between average cost and computation time, as previously mentioned, executing IRA at the initial time step is the primary source of both cost reduction and increased computation time.

Table S.3. Average cost and computation time using the kinematic vehicle model with different switching time t_s ($\alpha = 0.2$).

t_s	0 (ARA)	1	6	11	16	20 (IRA)
Average cost	15.13	5.06	3.74	2.90	2.89	2.89
Average computation time	0.078	0.118	0.121	0.129	0.129	0.131

D. Sensitivity analysis of the calibration set division

Table S.4 shows the average cost, average computation time and collision avoidance rate using the kinematic vehicle model and E2E-CP-ARA ($\alpha = 0.2$) with 10 different random calibration set divisions. Specifically, for each experiment, we randomly divide the calibration dataset D_{cal} into D_{cal}^1 and D_{cal}^2. It can be observed that, for the ten random experiments, the standard deviation of the average cost is 0.643, and the coefficient of variation is 4.2%, indicating relatively low volatility. For the collision avoidance rate, its volatility is only 2.3%, and all values do not exceed the given tolerance (80%). Therefore, the proposed method is insensitive to the calibration set division.

Table S.4. Average cost, average computation time and collision avoidance rate using the kinematic vehicle model and E2E-CP-ARA ($\alpha = 0.2$) with 10 different random calibration set divisions.

Division index	1	2	3	4	5	6	7	8	9	10
Average cost	15.13	14.78	15.11	16.03	15.96	14.37	14.60	15.73	15.64	16.19
Average computation time	0.078	0.078	0.079	0.077	0.072	0.080	0.065	0.074	0.086	0.084
Collision avoidance rate	89.1%	89.2%	90.5%	88.2%	88.6%	88.4%	90.5%	89.2%	89.3%	89.9%

E. An extension using the normalized nonconformity score in Stamouli et al. (2024)

Stamouli et al. (2024) proposed a normalized nonconformity score, which can improve performance compared to S-CP (Lindemann et al., 2023). In this section, we incorporate this normalized nonconformity score into E2E-CP to further enhance its performance as follows. First, we still follow the content outlined prior to Section 4.1. Instead of using the

original nonconformity score as in Section, we can redefine the nonconformity score at time τ as follows to replace (6).

$$\begin{aligned} R_\tau &= \max_{t=0,\dots,\tau-1} \left\{ \frac{\|Y_\tau - \hat{Y}_{\tau|t}\|}{\sigma_{\tau|t}} \right\} \\ R_\tau^{(i)} &= \max_{t=0,\dots,\tau-1} \left\{ \frac{\|Y_\tau^{(i)} - \hat{Y}_{\tau|t}^{(i)}\|}{\sigma_{\tau|t}} \right\} \quad \forall i = 1, ..., K \end{aligned} \tag{S2}$$

where

$$\sigma_{\tau|t} = \max_{j \in \mathcal{I}_{train}} \|Y_\tau^{(j)} - \hat{Y}_{\tau|t}^{(j)}\|, \quad \forall t,\ \tau > t \tag{S3}$$

where $\mathcal{I}_{train} = \{j : Y^{(j)} \in D_{train}\}$ denotes the set of indices of the data in the training set D_{train}. We note that, compared to the nonconformity score in Stamouli et al. (2024), we separate the nonconformity score at each time τ, which facilitates the reallocation of the risk at each time step. Similarly, given an allocated risk α_τ for future time τ, the random variables $R_\tau, R_\tau^{(1)}, ..., R_\tau^{(K)}$ are exchangeable and the prediction region with coverage guarantee is derived according to Lemma 3.3 as follows.

$$\mathbb{P}\left\{ \max_{t=0,\dots,\tau-1} \left\{ \frac{\|Y_\tau - \hat{Y}_{\tau|t}\|}{\sigma_{\tau|t}} \right\} \le C_\tau^{1-\alpha_\tau} \right\} \ge 1 - \alpha_\tau \tag{S4a}$$

$$C_\tau^{1-\alpha_\tau} = Quantile_{1-\alpha_\tau}(R_\tau^{(1)}, ..., R_\tau^{(K)}, \infty) \tag{S4b}$$

Based on the $(1-\alpha_\tau)$-coverage prediction region defined in (S4a), the individual chance constraint $\mathbb{P}\{c(x_\tau, Y_\tau) \ge 0\} \ge 1 - \alpha_\tau$ can be reformulated as the following lemma.

Lemma E.1. *(chance constraint) If Assumptions 3.1 and 3.2 hold, the constraint function c is L-Lipschitz continuous and $\max_{0\le s\le t}\{c(x_\tau, \hat{Y}_{\tau|t}) - LC_{\tau|t}^{1-\alpha_\tau}\} \ge 0$ is satisfied where $C_{\tau|t}^{1-\alpha_\tau} = \sigma_{\tau|t} C_\tau^{1-\alpha_\tau}$, then the individual chance constraint $\mathbb{P}\{c(x_\tau, Y_\tau) \ge 0\} \ge 1 - \alpha_\tau$ is satisfied.*

Proof. According to the $(1-\alpha_\tau)$-coverage prediction region defined in S4a, we can obtain that

$$\mathbb{P}\left\{ \bigcap_{t=0}^{\tau-1} \left\{ \frac{\|Y_\tau - \hat{Y}_{\tau|t}\|}{\sigma_{\tau|t}} \right\} \le C_\tau^{1-\alpha_\tau} \right\} \ge 1 - \alpha_\tau \tag{S5}$$

According to that fact $t \le \tau - 1$ and the definition, we have the following inequality.

$$\mathbb{P}\left\{ \bigcap_{t=0}^{t} \left\{ \|Y_\tau - \hat{Y}_{\tau|t}\| - C_{\tau|t}^{1-\alpha_\tau} \right\} \le 0 \right\} \ge \mathbb{P}\left\{ \bigcap_{t=0}^{\tau-1} \left\{ \|Y_\tau - \hat{Y}_{\tau|t}\| - C_{\tau|t}^{1-\alpha_\tau} \right\} \le 0 \right\} \ge 1 - \alpha_\tau \tag{S6}$$

Based on (S6), we can further obtain the following inequality.

$$\mathbb{P}\left\{ C_{\tau|s}^{1-\alpha_\tau} - \|Y_\tau - \hat{Y}_{\tau|s}\| \ge 0 \right\} \ge 1 - \alpha_\tau, \quad \forall s = 0, ..., t \tag{S7}$$

Note that the function c is L-Lipschitz continuous, the following inequality is obtained.

$$\|c(x_\tau, Y_\tau) - c(x_\tau, \hat{Y}_{\tau|t})\| \le L\|Y_\tau - \hat{Y}_{\tau|t}\| \Longrightarrow c(x_\tau, Y_\tau) \ge c(x_\tau, \hat{Y}_{\tau|t}) - L\|Y_\tau - \hat{Y}_{\tau|t}\| \tag{S8}$$

If the constraint $\max_{0\le s\le t}\{c(x_\tau, \hat{Y}_{\tau|t}) - LC_{\tau|t}^{1-\alpha_\tau}\} \ge 0$ is satisfied, we have the following inequality.

$$\exists s = 0, ..., t \quad c(x_\tau, Y_\tau) \ge L(C_{\tau|s}^{1-\alpha_\tau} - \|Y_\tau - \hat{Y}_{\tau|s}\|) \tag{S9}$$

By combining (S7) and (S9), we ultimately obtain $\mathbb{P}\{c(x_\tau, Y_\tau) \ge 0\} \ge 1 - \alpha_\tau$. □

Finally, it is sufficient to replace constraint (11e) in the TO problem (11) with $\max_{0\le s\le t}\{c(x_\tau, \hat{Y}_{\tau|t}) - LC_{\tau|t}^{1-\alpha_\tau}\} \ge 0$. For the posterior probability calculation and risk allocation method, since we have separated the nonconformity score at each time step τ, our proposed framework remains fully applicable. It is important to note that, as described in Section B, the constraint $\max_{0\le s\le t}\{c(x_\tau, \hat{Y}_{\tau|t}) - LC_{\tau|t}^{1-\alpha_\tau}\} \ge 0$ introduces mixed-integer variables into the TO problem, which significantly increases the solution time, especially when using the IRA method and dealing with nonlinear systems.

References

Alahi, A., Goel, K., Ramanathan, V., Robicquet, A., Fei-Fei, L., and Savarese, S. Social lstm: Human trajectory prediction in crowded spaces. In *Proceedings of the IEEE conference on computer vision and pattern recognition*, pp. 961–971, 2016.

Dixit, A., Lindemann, L., Wei, S. X., Cleaveland, M., Pappas, G. J., and Burdick, J. W. Adaptive conformal prediction for motion planning among dynamic agents. In *Learning for Dynamics and Control Conference*, pp. 300–314. PMLR, 2023.

Lekeufack, J., Angelopoulos, A. N., Bajcsy, A., Jordan, M. I., and Malik, J. Conformal decision theory: Safe autonomous decisions from imperfect predictions. In *2024 IEEE International Conference on Robotics and Automation (ICRA)*, pp. 11668–11675. IEEE, 2024.

Lindemann, L., Cleaveland, M., Shim, G., and Pappas, G. J. Safe planning in dynamic environments using conformal prediction. *IEEE Robotics and Automation Letters*, 2023.

Stamouli, C., Lindemann, L., and Pappas, G. Recursively feasible shrinking-horizon mpc in dynamic environments with conformal prediction guarantees. In *6th Annual Learning for Dynamics & Control Conference*, pp. 1330–1342. PMLR, 2024.